# Emplacement of a silicic lava dome through a crater glacier: Mount St Helens, 2004–06

Joseph S. WALDER, Richard G. LaHUSEN, James W. VALLANCE, Steve P. SCHILLING

*United States Geological Survey, Cascades Volcano Observatory, 1300 Southeast Cardinal Court, Vancouver, Washington WA 98683-9589, USA*
*E-mail: jswalder@usgs.gov*

**ABSTRACT. The process of lava-dome emplacement through a glacier was observed for the first time after Mount St Helens reawakened in September 2004. The glacier that had grown in the crater since the cataclysmic 1980 eruption was split in two by the new lava dome. The two parts of the glacier were successively squeezed against the crater wall. Photography, photogrammetry and geodetic measurements document glacier deformation of an extreme variety, with strain rates of extraordinary magnitude as compared to normal alpine glaciers. Unlike normal temperate glaciers, the crater glacier shows no evidence of either speed-up at the beginning of the ablation season or diurnal speed fluctuations during the ablation season. Thus there is evidently no slip of the glacier over its bed. The most reasonable explanation for this anomaly is that meltwater penetrating the glacier is captured by a thick layer of coarse rubble at the bed and then enters the volcano's groundwater system rather than flowing through a drainage network along the bed.**

## INTRODUCTION

Since October 2004, a lava dome has been emplaced first through, and then alongside, glacier ice in the crater of Mount St Helens, Washington state, US. The dome has been emplaced in a near-solid state, not as liquid magma solidifying at the Earth's surface (Vallance and others, in press. The crater glacier has been cut in half and the resulting ice bodies have been successively squeezed between the growing lava dome and the crater walls.

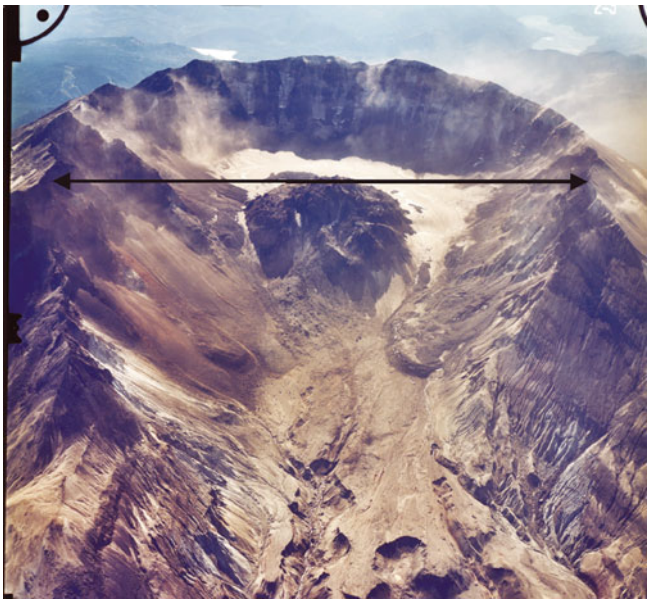

**Fig. 1.** Oblique view of Mount St Helens crater on 5 October 2000, looking south. Crater Glacier wraps around the 1980–86 lava dome. The eastern arm of the glacier is obscured by rock-avalanche debris; the western arm merges to the north of the lava dome with a rock-covered icy mass shed off the west crater wall. Crater width is about 2 km.

Several examples of lava-dome emplacement into ice have previously been inferred from geological- and geophysical evidence: silicic lava domes emplaced beneath the caldera glacier of Volcán Sollipulli, Chile (Gilbert and others, 1996); a dome-like rhyolite body emplaced subglacially in Iceland and since exhumed (Tuffen and others, 2001); and a lava dome emplaced through the caldera glacier of Great Sitkin volcano, Alaska, in 1945 (Simons and Mathewson, 1955, plate 6). Our data are the first to actually document glacier response to lava-dome emplacement. The concise account here is supplemented by Walder and others (in press), which includes a lengthy photographic chronology.

## PECULIAR NATURE OF THE CRATER GLACIER

The cataclysmic eruption of 18 May 1980 beheaded – and in some cases completely destroyed – the glaciers that had previously existed on the flanks of Mount St Helens (Brugman and Meier, 1981), and created a crater breached on the north side. A lava dome (Fig. 1) grew episodically in the crater until mid-1986 (Swanson and Holcomb, 1989). The crater floor between the crater walls and the 1980s lava dome, where any crater glacier would, by definition, have to grow, is a dangerous place to work owing to frequent rock and snow avalanches from the crater walls. Thus our discussion of when a crater glacier came into existence relies upon photographic evidence.

As of mid-1988 (Mills, 1992), material shed from the crater walls had accumulated to a thickness of as much as 60–80 m on the south crater floor. Accumulated material was about 60% by volume rock debris (much of it of gravel and cobble size) with interstitial snow, and did not seem to be flowing. The first reasonably clear evidence for flow (in the way of crevasses) was revealed by aerial photographs taken in September 1996 (Schilling and others, 2004). The surface

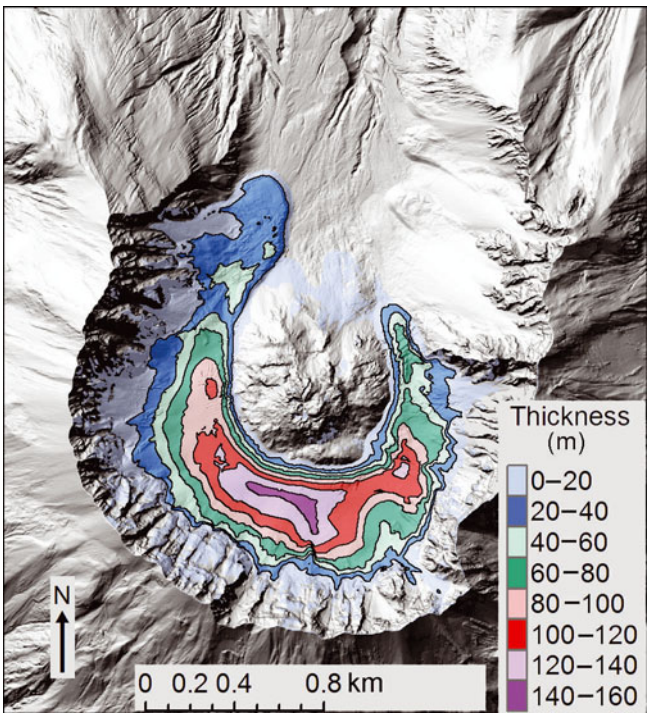


**Fig. 2.** Thickness of material accumulated on the crater floor between October/November 1986 and September 2003. Background is a shaded relief map constructed from the September 2003 digital elevation model. The 1980–86 lava dome is in the center. The October/November 1986 surface is approximately the glacier bed and the isopachs approximately represent glacier thickness, except north of the dome where talus shed by the dome has accumulated.

area of Crater Glacier was about 0.1 km$^2$ at that time, but had increased to about 1 km$^2$ by September 2000. Schilling and others (2004) determined by differencing digital elevation models (DEMs) that $1.2 \times 10^8$ m$^3$ of material (about 30% being rock debris) had accumulated on the crater floor between 1980 and September 2000, with thickness locally as great as 200 m. The general picture presented by the Mills (1992) and Schilling and others (2004) studies, along with our own field observations, is that the lowermost (deepest) part of the crater-floor fill consists primarily of rock-avalanche debris and should not be considered glacier ice; the uppermost (shallowest) part of this fill, however, contains rock debris only in relatively thin, discontinuous layers, and may reasonably be called 'dirty' firn and ice.

As the focus here and in the companion paper (Price and Walder, 2007) is on deformation and flow of Crater Glacier in response to the episode of lava-dome growth that began in September 2004, we exclude from consideration, as best we can, the lowermost, rock-rich, crater-floor fill. We do this by setting the glacier bed to be the crater-floor surface defined by DEMs for 12 October 1986 and 12 November 1986. This is an approximate but reasonable choice (Walder and others, in press) because (1) the rate of accumulation of rock debris in the crater decreased markedly after 1986; (2) 1986 marks the end of the last dome-growth episode, so accumulation after 1986 occurred within a basin with reasonably stable boundaries and (3) much of the interstitial ice within the lowest, rock-rich crater-fill material has probably melted and not been replaced by ice intruding from above. With the 1986 surface thus defined as the nominal glacier bed, we then differenced 2003 and 1986 DEMs to calculate glacier thickness shortly before the start of the 2004 eruption (Fig. 2). Using the Mills (1992) and Schilling and others (2004) figures for rock-debris accumulation, we estimate that the glacier defined in this way has an average rock content of 15% by volume.

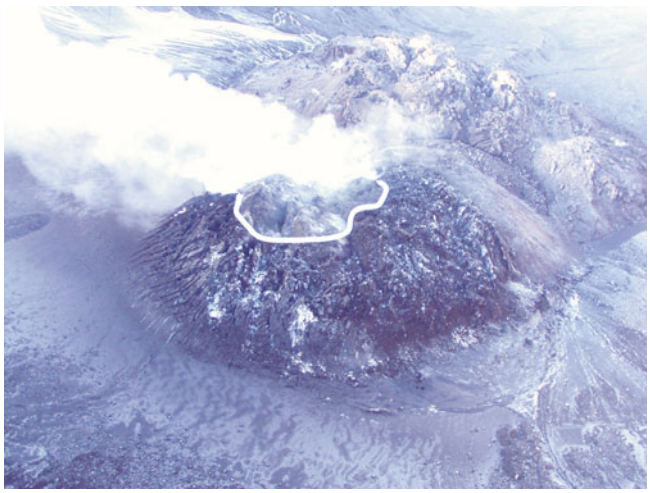

**Fig. 3.** Upwarped firn and ice around the margins of lava-dome spine 2. Line shows approximate spine–glacier contact. View to the north on 13 October 2004, with the 1980–86 lava dome in the background. Photograph courtesy of S. Konfal.

## METHODS

We documented eruptive effects on Crater Glacier by photography, photogrammetry and single-frequency Global Positioning System (GPS) stations on the glacier. Hazards posed by an erupting volcano severely restricted fieldwork in the crater. The helicopter-deployed GPS stations were designed for and dedicated to ground-deformation monitoring and were available for glacier monitoring only sporadically. Station positions were determined from short baseline differential fixed static solutions sampled at 10 second intervals over a 25 minute period every hour. Accuracy of individual solutions was approximately 20 mm in the horizontal and 50 mm in the vertical. A running-median filter was applied to solutions to remove spikes.

## MORPHOLOGICAL CHANGES IN CRATER GLACIER SINCE OCTOBER 2004

One of the first indirect signs of dome growth was the formation of a bulge in the south part of Crater Glacier during the last few days of September 2004. An explosion on 1 October 2004 excavated a hole in the glacier. As the eruption proceeded, the south part of Crater Glacier was eventually punctured by a rock 'spine' surrounded by rubble (the latter perhaps comprising the unconsolidated material that underlies the glacier). The lava dome as it existed as of 1 August 2006 comprised a complex of seven such spines that extruded sequentially from the same general vent area (Vallance and others, in press). All spines have been extruded in the solid state. Spine 3, which began to be extruded in late October 2004, grew preferentially southward, developing a 'whaleback' form and pushing aside firn and ice like a bow wave preceding a ship through water

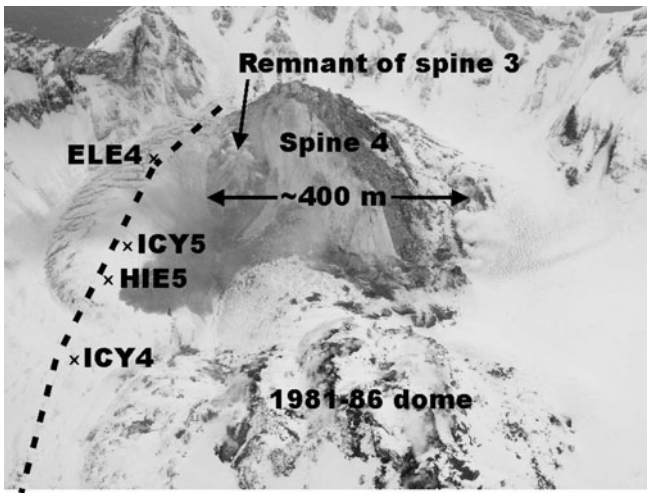


**Fig. 4.** ECG and new lava dome as of 10 April 2005. View is southeast. Dashed curve is approximately the line of section for glacier bed and surface as shown in Fig. 6. GPS station locations indicated by crosses. Photograph courtesy of J.J. Major, USGS.

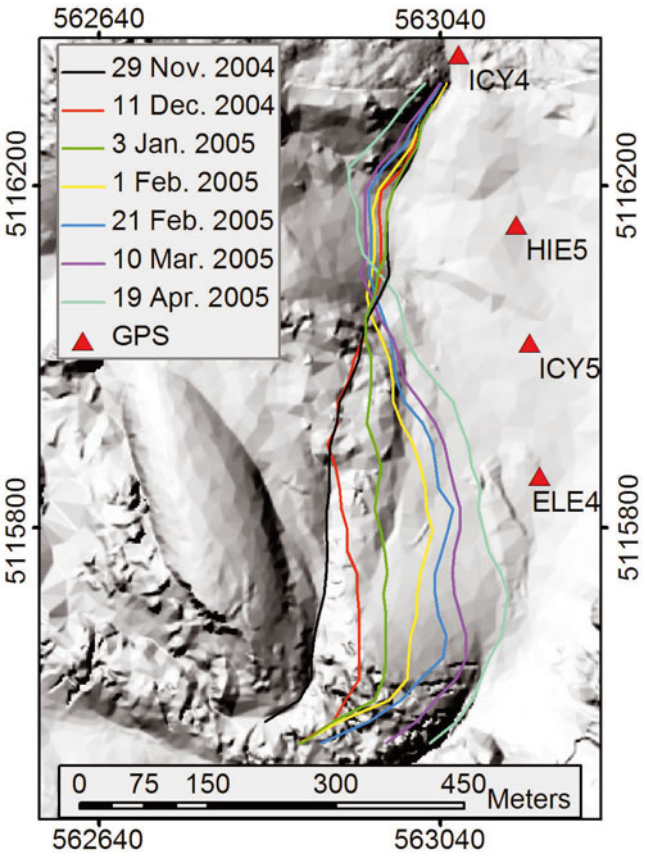


**Fig. 5.** Migration of contact between new lava dome and ECG from 29 November 2004 to 19 April 2005. Contacts were determined from DEMs, with an error of about 5 m. Background is a shaded relief map for 29 November 2004. North is to the top, and coordinates are UTM zone 10 easting and northing. Eastward migration of the rock–glacier contact for northing $<\sim$5116050 reflects growth of the new lava dome, which not only caused the glacier locally to thicken but also enhanced ice flow to the north. Ice encroached upon the margin of the old (1981–86) lava dome, as reflected by an apparent westward migration of the rock–glacier contact for northing $>\sim$5116050.

(Fig. 3). After spine 3 ran into the south crater wall in mid-November 2004, Crater Glacier was, for all practical purposes, split into two parts referred to as East Crater Glacier (ECG) and West Crater Glacier (WCG). Spine 3 spread to the east until late December 2004, then decrepitated and was shouldered aside by spine 4 – another 'whaleback' – which grew until mid-April 2005. ECG was effectively caught in a vise formed by the whaleback spines and the east crater wall (Fig. 4).

Glacier-surface features showed up very clearly during the drought of winter 2004/05. As spines 3 and 4 grew, the ECG surface buckled, with east–west trending crevasses forming parallel to the direction of dome spreading. Comparison of sequential aerial photographs showed that between mid-November 2004 and mid-April 2005, the dome–ECG contact migrated laterally by as much as 200–250 m (Fig. 5), corresponding to an average migration rate of about 1 m d$^{-1}$. The glacier locally doubled in thickness during this period of time (Fig. 6), with the surface rising at a rate of about 0.6 m d$^{-1}$. Since spine 4 stopped growing in mid-April 2005, the dome–ECG contact has not moved and the glacier has thinned in its upper reach and thickened in its lower reach as normal flow processes have redistributed ice mass. The ECG terminus became steeper and advanced by 80–90 m between 19 April and 15 December 2005.

Spine 6 developed on the west side of the lava-dome complex beginning in late June 2005, and a part of WCG began to bulge and fracture in much the same way as had happened with ECG. Spine 6 was superseded and overridden by spine 7 beginning in early October 2005, but the push on WCG continued (Fig. 7). Comparison of DEMs reveals that between 15 June and 15 December 2005, the dome–WCG contact migrated laterally by as much as 200–250 m (Fig. 8), corresponding to an average migration rate of about 1 m d$^{-1}$. WCG locally doubled in thickness during this period (Fig. 9). WCG continues to be squeezed by the growing lava dome as of 1 August 2006.

The change in glacier volume during the course of the eruption can be determined by comparing DEMs for different dates (Walder and others, in press). The estimated volume decrease from the start of the eruption in October 2004 to October 2005 (approximately equivalent to the period between the end of one ablation season and the end of the next) represents a loss of about 0.2 m$^3$ s$^{-1}$, but the error in this estimate is larger than this. The eruption has clearly been unaffected by a process commonly associated with volcano–glacier interactions: rapid meltwater generation (Major and Newhall, 1989). This is unsurprising; the eruption has been predominantly quiescent and not explosive, so scouring of the glacier surface by hot fragmental flows has been negligible. Moreover, the spines have been extruded in a solid state, with surface temperature well below the solidus, and well insulated from the glacier by a blanket of rubble (Vallance and others, in press).

## DYNAMIC RESPONSE OF THE GLACIER

### East Crater Glacier

Although we have no data directly bearing on surface speed before the 2004 eruption began, a very rough 'balance velocity' $U_b$ can be estimated as

$$U_b \approx \frac{L}{H} b,$$

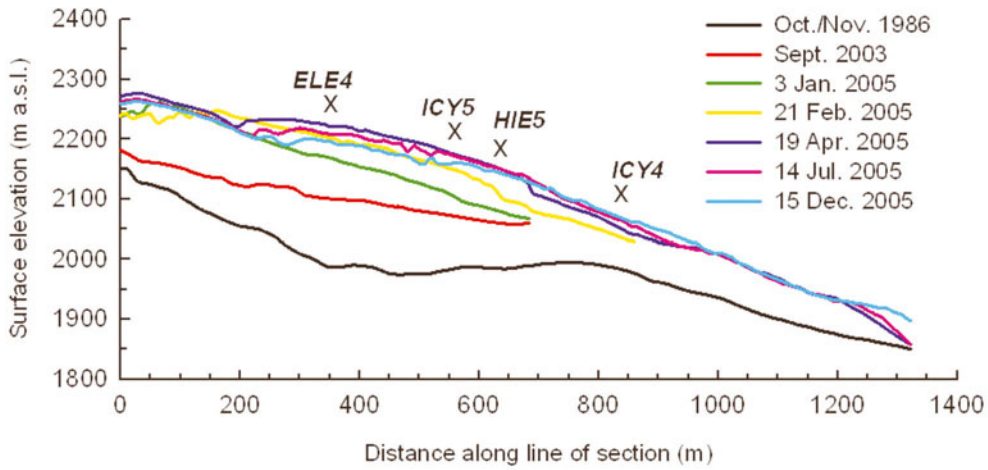


**Fig. 6.** Change in surface elevation of ECG based on time-sequential DEMs. Line of section and GPS station locations are shown in Figures 4 and 5. (Note that GPS station ICY4 was adjacent to the 1980–86 lava dome and thus north of the part of East Crater Glacier that was squeezed.) The 1986 profile is approximately the glacier bed. The 2003 profile should be within a few meters elevation of the glacier surface at the beginning of the current eruption. Not all DEMs extend to the glacier terminus.

where $L$ is the distance from the 'headwall' of ECG (i.e. the south crater wall) to the ECG terminus, $H$ is the average pre-eruption ice thickness in this reach and $b$ is the long-term mass balance. With $L \approx 1.3$ km, $H \approx 80$ m (see Fig. 6) and $b \approx 4\,\mathrm{m\,a^{-1}}$ (from a total ice accumulation of about $80 \times 10^6\,\mathrm{m^3}$ over an area of about $1\,\mathrm{km^2}$ in 20 years), we find $U_b \approx 0.18\,\mathrm{m\,d^{-1}}$ which corresponds to a surface speed of about $0.23\,\mathrm{m\,d^{-1}}$ for ice with the flow-law exponent $n = 3$ (van der Veen, 1999). Interestingly, this is comparable to the speed of station ICY4, which was down-glacier of the domain squeezed by the lava dome, on ice about 70 m thick and not far from the ECG terminus (Fig. 10). Compare with ICY5, located about 300 m up-glacier of ICY4: ICY5 is within the reach being squeezed by dome growth (Figs 4 and 5), on ice about 150 m thick and moved about $1.3\,\mathrm{m\,d^{-1}}$, or about 4 times as fast as ICY4. If deformation were only by simple shear and reflected a balance between gravitational driving stress and drag on the glacier bed and sides, the difference in surface velocity between ICY4 and ICY5 should have been a factor of about $(150/70)^{n+1} = 21$ for a flow-law exponent $n = 3$ (van der Veen, 1999). Moreover, owing to the non-linear rheology of glacier ice (van der Veen, 1999), the

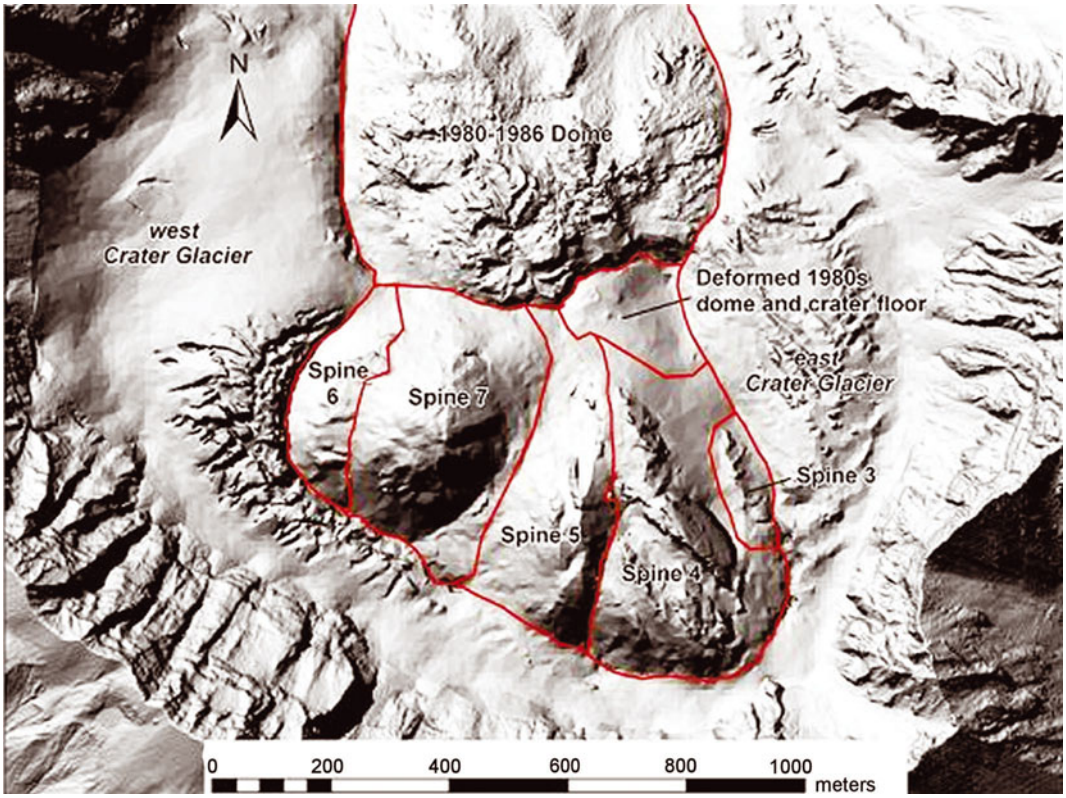


**Fig. 7.** The spines that comprise the lava dome are indicated on this shaded relief map constructed from an aerial photograph of 15 December 2005. Spines 1 and 2 had completely crumbled by this date, and only a remnant of spine 3 remained (compare with Fig. 4).

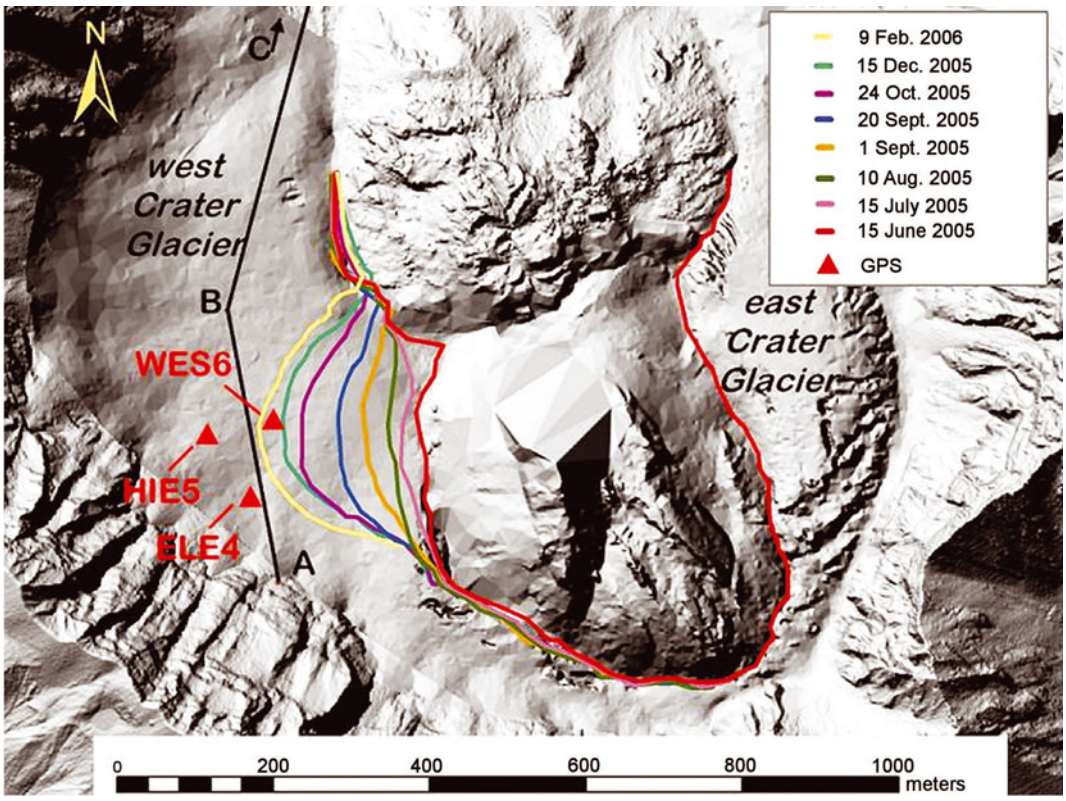


**Fig. 8.** Migration of contact between lava dome and WCG during the period 15 June to 15 December 2005. Contact position was determined from DEMs, with an error of about 5 m. The background is a shaded relief map for 15 June 2005; missing data reflect where ground surface was obscured by steam plume.

squeeze exerted on ECG by the growing lava dome should have 'softened' the ice near ICY5 and made the difference in speed from ICY4 to ICY5 even greater. The driving stress was clearly not balanced by drag; the glacier near ICY4 acted as a dam to restrain outflow of the 'soft' ice farther up-glacier, resulting in a large longitudinal stress gradient (Price and Walder, 2007).

Gross average strain rates associated with the squeeze exerted on ECG can be estimated, in part, by considering the rate of eastward migration of the dome–glacier contact and the rate of glacier-surface uplift. Dividing the rate of eastward migration of the dome–glacier contact near ELE4 (Fig. 5) by the glacier width (about 300 m), the average rate of contact migration for the period 11 December 2004 to 3 January 2005 corresponds to a 'squeeze' strain rate of about $-0.006\,\mathrm{d}^{-1}$. For the period 3 January to 19 April 2005, the squeeze strain rate was about $-0.0036\,\mathrm{d}^{-1}$. To put the ECG strain rate values into perspective, consider ice moving through a valley constriction at a rate of $100\,\mathrm{m\,a}^{-1}$ with the valley narrowing by 25% over a length of 1 km – arguably a rather severe constriction. The lateral strain rate in this case would be $-0.0001\,\mathrm{d}^{-1}$ or about 1–3% of the lateral strain rate associated with squeezing of the ECG.

The strain rate associated with glacier thickening for the period 3 January to 19 April 2005 can be roughly estimated (Fig. 6) at about $(0.6\,\mathrm{m\,d}^{-1})/100\,\mathrm{m} \approx 0.006\,\mathrm{d}^{-1}$ near the ECG 'centerline'. There were never two GPS units simultaneously on the reach being squeezed, so we cannot estimate the longitudinal strain rate within that domain. The longitudinal strain rate in the domain bounded by ICY5 and

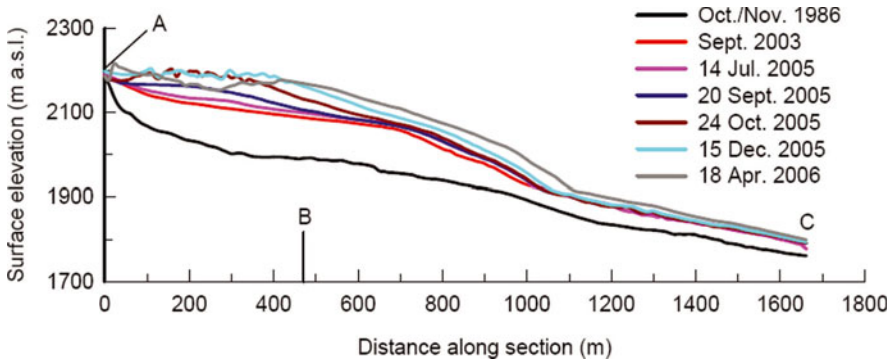


**Fig. 9.** Change in surface elevation of WCG, based on time-sequential DEMs. Line of section is shown in Figure 8. The 1986 profile is approximately the glacier bed. The 2003 profile should be within a few meters elevation of the glacier surface at the beginning of the current eruption.

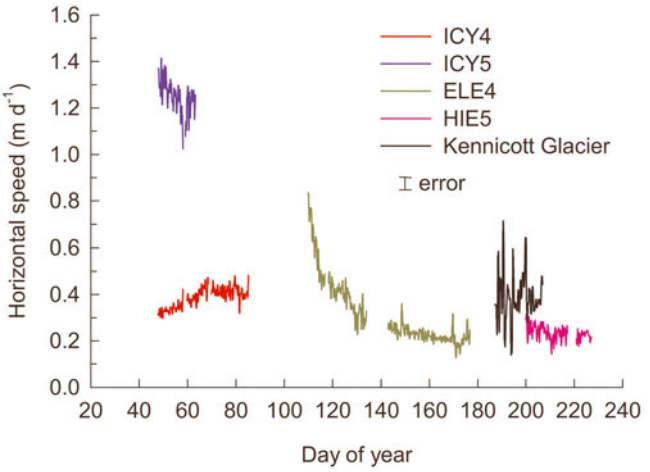


**Fig. 10.** Horizontal speed of ECG GPS stations. ICY4 and ICY5 were on the glacier while lava-dome spine 4 was expanding eastward. ELE4 was fortuitously placed on the glacier about the time that spine 4 stopped growing. HIE5 was on the glacier in mid-summer. Azimuth of motion for all stations was within 18° of north. For comparison we show surface-speed data (adapted from Anderson and others, 2005) for a target on Kennicott Glacier, a temperate valley glacier in Alaska, during the year 2000. The record for Kennicott Glacier shows large amplitude, commonly diurnal fluctuations not seen at ECG.

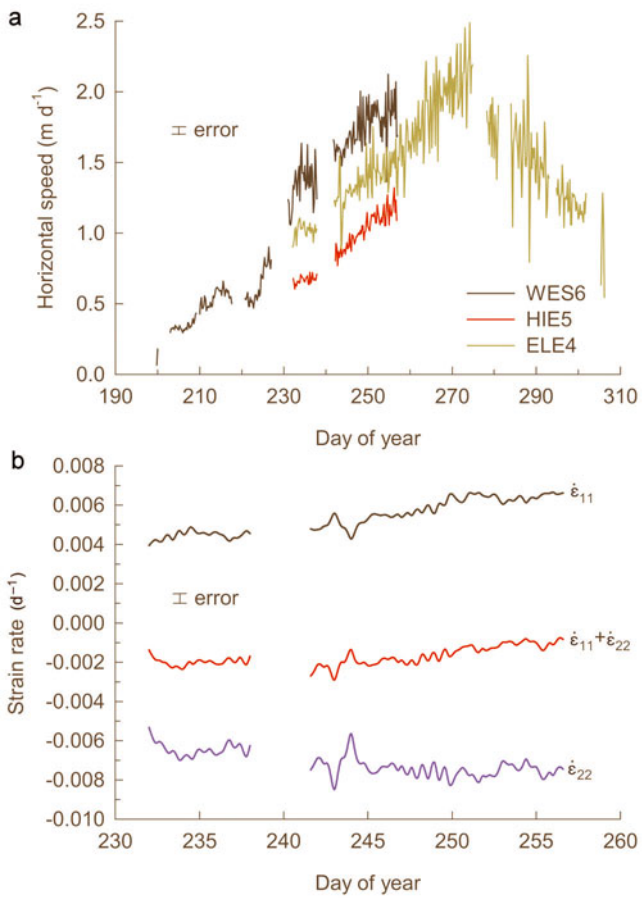


**Fig. 11.** GPS-derived motion data for WCG. (a) Horizontal speeds. The change in trend of ELE4 occurred at about the same time that spine 6 stopped growing and spine 7 began growing. As with the ECG record (Fig. 10), diurnal speed fluctuations are not seen at WCG; (b) Principal strains in the horizontal plane. The direction of maximum extension $\dot{\varepsilon}_{11}$ is N10E; the direction of maximum compression $\dot{\varepsilon}_{22}$ is N80W.

ICY4 can be estimated as the difference in flow speed divided by separation, or $(-0.9\,\mathrm{m\,d^{-1}})/350\,\mathrm{m} \approx -0.0026\,\mathrm{d^{-1}}$; a value otherwise known only from surge fronts (Kamb and others, 1985).

## West Crater Glacier

Approximate GPS station positions are shown in Figure 8; displacement rates are shown in Figure 11a. WCG stations recorded the response of the glacier to westward dome growth. The peak in speed of ELE4 at about day 273 (30 September 2005) occurred just a few days before the appearance of spine 7 east of spine 6 (Fig. 7; Vallance and others, in press) and probably reflects a change in the stresses applied to WCG by the dome. During the 23-day period when the records overlapped, all three stations rather smoothly accelerated, with differences in azimuth of motion reflecting the local direction of dome growth. Displacement records for the overlap period were analyzed to determine direction and magnitude of the principal strain rates within the (approximately horizontal) plane determined by the three stations. Magnitudes of principal horizontal strain rates increased slowly, with their sum consistently negative at about $-0.002\,\mathrm{d^{-1}}$ (Fig. 11b). Making the plausible interpretation that surface uplift represents thickening of the glacier, vertical strain rate can be estimated as the average uplift rate divided by the glacier thickness, or about $(0.25\,\mathrm{m\,d^{-1}})/120\,\mathrm{m} = 0.002\,\mathrm{d^{-1}}$. The sum of the three principal strain rates was thus locally near zero, consistent with bulk incompressibility.

## INFERENCES ABOUT GLACIER AND VOLCANO HYDROLOGY

Measurements on many glaciers have shown systematic differences in surface speed during the ablation season when compared to during winter. Surface speed in summer is higher than in winter, and large diurnal variations in surface speed are common (Fountain and Walder, 1998). Moreover, pulses of increased surface speed are commonly observed at the beginning of the melt season (Anderson and others, 2004). As the creep component of glacier motion should be reasonably constant, variations in surface speed are customarily thought to reflect variations in sliding speed, which is modulated by meltwater at the bed (for example, Harper and others, 2002). ECG data, however (Fig. 10), show neither acceleration with the onset of the melt season nor a clear diurnal signal; WCG data for summer 2005 (Fig. 11a) similarly lack any diurnal signal. Evidently these are temperate glaciers that do not slide over their beds.

We suggest that the absence of sliding is related to the peculiar nature of the crater glaciers and their substrate. Regardless of exactly where the effective glacier bed is located, it is certainly very rough owing to the extreme coarseness of the rockfall debris shed from the crater walls since the 1980 eruption; furthermore, the basal ice must contain a lot of the same coarse rock debris. There must be a great deal of frictional resistance to basal sliding unless water pressure at the bed is very close to overburden pressure (Cohen and others, 2005). But such high water pressure is improbable. The glacier – regardless of exactly where its base is – overlies a layer of rock-avalanche debris that is tens

of meters thick. Much of this debris is likely to be ice-free since geothermal heat flow will have melted interstitial ice, and flow of the overlying ice down into the rubble will be very slow (Walder and others, in press). Moreover, the volcanic edifice beneath the avalanche deposits is geologically complex, consisting of multiple lava flows, pyroclastic and lahar deposits and other fragmental deposits (Crandell, 1987). Thus, water probably flows either out of the crater through the rubble layer or downward into the volcano's groundwater system, rather than moving along the glacier bed through a pressurized drainage system. This situation would keep pore-water pressure within the rubble layer relatively low and thereby also preclude pervasive shear deformation within the rubble. In support of this interpretation, we note that there are no outlet streams at either ECG or WCG termini, but rather springs and seeps further downslope. Moreover, occasional discharge measurements in Loowit Creek, which drains the crater, have shown no evidence of systematically elevated streamflow during the eruption (K.R. Spicer, personal communication, 2006).

## CONCLUSIONS

The eruption of Mount St Helens that began in fall 2004 presented us with the first-ever opportunity to observe and document emplacement of a lava dome through glacier ice. Dome growth cut the crater glacier into two parts, each of which was successively squeezed against the crater wall, with strain rates of extraordinary magnitude when compared to normal alpine temperate glaciers. GPS-derived motion records confirm that the crater glaciers are fundamentally unlike normal temperate glaciers, in that there is strong evidence for the absence of basal sliding. The most reasonable explanation for this anomaly is that meltwater reaching the glacier bed enters the volcano's groundwater system rather than flowing toward the glacier terminus through a drainage network along the bed. The eruption has not caused rapid melting of the crater glacier. Sufficiently prolonged dome growth could of course completely eliminate ice from the crater (and indeed completely eliminate the crater itself). Glaciers at Mount St Helens come and go, modulated by the style and rhythm of eruptive behavior.

## ACKNOWLEDGEMENTS

DEMs were prepared by J. Messerich of the US Geological Survey Photogrammetric Lab, Denver, Colorado. Comments by an anonymous reviewer improved the manuscript.

## REFERENCES

Anderson, R.S. *and 6 others*. 2004. Strong feedback between hydrology and sliding of a small alpine glacier. *J. Geophys. Res.*, **109**(8). (10.1029/2004JF000120.)

Anderson, R.S., J.S. Walder, S.P. Anderson, D.C. Trabant and A.G. Fountain. 2005. The dynamic response of Kennicott Glacier to the Hidden Creek Lake outburst flood. *Ann. Glaciol.*, **40**, 237–242.

Brugman, M.M. and M.F. Meier. 1981. Response of glaciers to eruptions of Mount St. Helens. *In* Lipman, P. and Mullineaux, D.R. *eds The 1980 Eruption of Mount St. Helens. USGS Professional Paper,* **1250**, 743–756.

Cohen, D., N. Iverson, T. Hooyer, U. Fischer, M. Jackson and P. Moore. 2005. Debris-bed friction of hard-bedded glaciers. *J. Geophys. Res.,* **110**(5). (10.1029/2004JF000228.)

Crandell, D.R. 1987. Deposits of pre-1980 pyroclastic flows and lahars from Mount St. Helens volcano. US Geol. Surv. Prof. Paper 1444, Washington.

Fountain, A.G. and J.S. Walder. 1998. Water flow through temperate glaciers. *Rev. Geophys.,* **36**(3), 299–328.

Gilbert, J. *and 6 others*. 1996. Non-explosive, constructional evolution of the ice-filled caldera at Volcán Sollipulli, Chile. *Bull. Volcanol.,* **58**(1), 67–83.

Harper, J.T., N.F. Humphrey and M.C. Greenwood. 2002. Basal conditions and glacier motion during the winter/spring transition, Worthington Glacier, Alaska, U.S.A. *J. Glaciol.,* **48**(160), 42–50.

Kamb, B. *and 7 others*. 1985. Glacier surge mechanism: 1982–1983 surge of Variegated Glacier, Alaska. *Science,* **227**(4686), 469–479.

Major, J.J. and C.G. Newhall. 1989. Snow and ice perturbation during historical volcanic eruptions and the formation of lahars and floods. A global review. *Bull. Volcanol.,* **52**, 1–27.

Mills, H.H. 1992. Post-eruption erosion and deposition in the 1980 crater of Mount St Helens, Washington, determined from digital maps. *Earth Surf. Proc. Land.,* **17**(8), 739–754.

Price, S.F. and J.S. Walder. 2007. Modeling the dynamic response of a crater glacier to lava-dome emplacement: Mount St. Helens, Washington, USA. *Ann. Glaciol.*, **45**, 21–28.

Schilling, S.P., P. Carrara, R. Thompson and E. Iwatsubo. 2004. Posteruption glacier development within the crater of Mount St. Helens, Washington, USA. *Quat. Res.,* **61**(3), 325–329.

Simons, F.S. and D.E. Mathewson. 1955. Geology of Great Sitkin Island, Alaska. *US Geol. Surv. Bull.,* 1028-B, 21–43.

Swanson, D.A. and R. Holcomb. 1989. Regularities in growth of the Mount St. Helens dacite dome, 1980–1986. *In* Fink, J.H., *ed. Lava flows and domes: emplacement mechanisms and hazard implications*. IAVCEI Poceedings in Volcanology 2, 3–24.

Tuffen, H., J. Gilbert and D. McGarvie. 2001. Products of an effusive subglacial rhyolite eruption: Bláhnúkur, Torfajökull, Iceland. *Bull. Volcanol.,* **63**(2–3), 179–190.

Vallance, J.W., S.P. Schilling, R. Thompson, and J. Messerich. In press. Growth of the recumbent dome at Mount St. Helens, 2004–2005. *In* Sherrod, D.A. and W.E. Scott, *eds. A volcano rekindled: the first year of renewed eruption at Mount St. Helens, 2004–05*: US Geol. Surv. Prof. Paper.

van der Veen, C.J. 1999. *Fundamentals of glacier dynamics.* Rotterdam, etc., A.A. Balkema Publishers.

Walder, J.S., S.P. Schilling, J.W. Vallance and R.G.LaHusen. In press. Effects of lava dome growth on the crater glacier of Mount St Helens. *In* Sherrod, D.A. and W.E. Scott, *eds. A volcano rekindled: the first year of renewed eruption at Mount St. Helens, 2004–05*: US Geol. Surv. Prof. Paper.